

Enhanced Photo-Generated Carrier Transport Mechanism in an Excitonic Photocell

¹Uzoma Oduah, Department of Physics, University of Lagos, Nigeria

²Wu Yang, Optik Design, Technische Universität, Ilmenau, Germany

³Frederick Anyadubalu, Department of Physics, University of Lagos, Nigeria

⁴Victor Nwaekwu, Department of Physics, University of Lagos, Nigeria

¹uoduah@unilag.edu.ng

³anyadubalu.fred@yahoo.com

²yang.wu@tu-ilmenau.de

⁴nwavic123@gmail.com

Abstract— Enhanced photo-generated carrier transport mechanism in an excitonic photocell is presented in this research project. The developed photovoltaic device implements nanoparticles of magnetites isolated from magnetosomes of Magnetotactic Bacteria (MTB) for the efficient transport of excitons. By integrating nanoparticles of magnetite in the excitonic photocell, the overall efficiency and temperature stabilization of the device were enhanced. A panchromatic ruthenium complex sensitizer dye was applied to increase molar extinction coefficient in the solar cell. Applying Zinc Oxide (ZnO) nanowires an improved circulation of photo-generated carriers with trap diffusion was created maximizing transport efficiency. The operation of this device involves the use of MTB as vehicle for the acceleration of the photo-generated excitons for a speedy dissociation and conversion to electrical energy. The developed device achieved a fill factor of 0.82 and overall efficiency of 13.2% attributed to the MTB. The availability of the device materials makes it feasible for mass production.

Index Terms— Magnetotactic Bacteria; Solar cell; Photocell; Exciton; Photovoltaic.

1.0 INTRODUCTION

The various technologies for conversion of incident photons to electricity are limited by recombination losses associated with the lifetime of excitons. The existing Organic Photovoltaic Cells includes the planar two-layer, Solar Cell introduced by Tang; the Dye-Sensitized Solar Cell (DSSC) by Grätzel; and the Bulk hetero-junction Solar Cell introduced by Sariciftci in collaboration with Heeger [1, 2, 3]. Although Silicon offers efficiency up to 18% to about 30%, these limits are yet to be exceeded for silicon even with different modifications of the device. Again the high cost of fabrication of the silicon device and the toxic chemicals associated with the production process are the major setbacks [4,5]. Dye sensitized solar cells are designed to replicate the natural process by which chlorophyll traps sunlight during photosynthesis. The DSSC suffers limitations such as poor efficiency index, complex production process leading to difficulty in commercialization. Considering the volume of research on silicon solar cell from inception to date and the current achieved minimal operational efficiency, compared to the sustained gradual growth in the DSSC efficiency, it is a good option to focus on DSSC technology. The features of DSSC are unique and advantageous over the solar cell devices that are based on crystalline or amorphous silicon. One striking advantage of DSSC is the ability of the components to be tunable such as the semiconducting oxide substrate, the dye, the electrolytes, the redox mediator and the counter electrodes. There are ongoing researches with various organic materials to position DSSC to be more competitive in the solar cell markets [6, 7, 8]. The target is to improve on the Incident Photon Conversion Efficiency (IPCE), enhance the cell durability, and reduce the cost of production applying an environmentally friendly technique. Several technologies have been used to improve on spectral absorbance by making modification in the dye, enhancing

the carrier transport mechanism, replacement of the liquid electrolyte with conducting polymers or ionic solids and other engineering of the semiconductor bandgap architecture [9, 10, 11]. Recent DSSC's are relatively low cost with nontoxic components that can easily be synthesized from abundant natural products.

2.0 MATERIAL AND METHODS

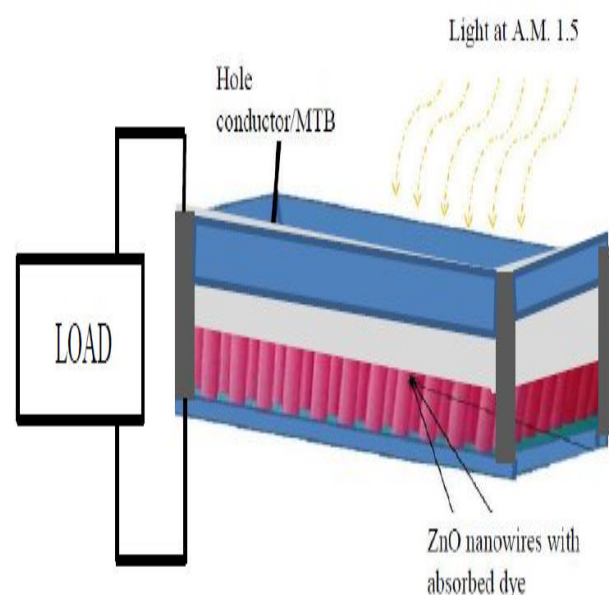


Figure 1. Excitonic Photocell with enhanced carrier transport mechanism

This research introduces a novel unique excitonic photocell described in Figure 1. It consists of a conducting glass, a

ruthenium dye as photo sensitizer, Zinc oxide nanowires loaded with nanoparticles of magnetite isolated from magnetosomes of MTB as charge carrier and electrodes. The device structure is designed to perform two functions which are firstly, photon absorption and secondly charge carrier transport. Photo excitation at the monolayer of the ruthenium dye results in the injection of electrons into the conduction band of the ZnO. The heart of this device is composed of nanoparticles of meso-porous with aggregate pore width of 2.50nm and oxide layer which allows accelerated electronic conduction to occur. The uniqueness of this device is on its characteristic photo-generated carriers transport mechanism in which excitons are accelerated by inbuilt magnetic field of nanoparticles of MTB. The speedy transport of excitons reduced the intrinsic recombination losses in this device which in turn enhanced the overall power conversion efficiency. Another desirable effect realized by incorporating the MTB in the device is that of temperature stability. This temperature stability is a serendipity attributed to the coherent transportation of the photo-generated excitons in the excitonic photocell. The steps taken in the processing of the materials used in the development of the DSSC are outlined as follows.

Samples of the MTB were collected from the Lagoon at University of Lagos, Nigeria, using screw top bottles. Then Magnetic Spirillum Growth Medium was used for the culture of the MTB. The culture method was according to the previous work done by Blakemore [12]. The magnetosomes of the MTB were then isolated and the crystal nanoparticles of the magnetite (Fe_3O_4) characterized using Selected Area Electron Diffraction (SAED) forms. Applying ionic interaction, the substrate was incorporated with isolated nanoparticles of the crystal magnetite. Transmission Electron Microscopy and Zeta potential were then used for the characterization of the magnetite nanoparticles. The processes deployed in the isolation of and characterization of the nanoparticles of magnetite described above followed the previous experimental protocols [13, 14, 15].

2.1 The ZnO Nanowires.

Nanowires of ZnO were used as photoanode of this solar cell. Nanowires of about 65nm diameter and length of $10\mu\text{m}$ were synthesized using substrate of Fluorine tin oxide (FTO, $\text{SnO}_2:\text{F}$) and then grown on Transparent Conductive Oxide [16, 17]. Here, ZnO nanowire is preferred to Titanium dioxide owing to the fact that it is easier to be synthesized with different nanostructures compared to Titanium dioxide. Also further advantages of ZnO nanowires over Titanium dioxide includes: the wider and direct bandgap about 3.37eV while Titanium dioxide has about 3.2eV, the excitation binding energy of (60 meV) which is higher compared to 4 meV of Titanium dioxide, and a higher electron mobility of about $200\text{ cm}^3\text{V}^{-1}\text{S}^{-1}$ compared to Titanium dioxide with $30\text{ cm}^3\text{V}^{-1}\text{S}^{-1}$. Applying Molecular Beam Epitaxy a narrow ZnO thin film was deposited uniformly on the silicon wafer. The temperature of the furnace was first raised to about 500°C using a ramping rate fixed at $20^\circ\text{C}/\text{min}$ until attaining an optimal temperature. Then a steady flow of about N_2 of 100 5ccm was blown into a tube while the pressure was kept constant at $1.0 \times 10^{-2}\text{Pa}$. Next, the furnace was cooled to a room temperature just after growth. The developed product material is ZnO nanowires, well aligned with a high density.

The product material is measured with 248 nm excimer, characterized using Scanning Electron Microscopy and also Photoluminescence Spectroscopy.

2.2 The Ruthenium Complex Dye.

Ruthenium dye is one of the amphiphilic homologues based on N-3 dye. The structure of the dye enhances the performance of the solar cell. The higher ground state introduced by the binding of moiety increases the electrostatic binding with the ZnO nanowires even at low pH levels. Through control of water-induced desorption in the dye, this complexes increases the stability of the device. Also, it achieves a better dye loading by attenuating electrostatic repulsion usually experienced in between layers of absorbed dye. Furthermore, the cathodical shifting of the oxidation potential in the complexes enhances its reversibility within the ruthenium III and ruthenium II couple, thereby improving on its stability. So, this panchromatic ruthenium, a complex light harvesting sensitizer developed with carboxylate terpyridyl combined with three thiocyanate groups linked as ligands achieved excellent incident photon conversion efficiencies in the solar cell [18, 19, 20, 21]. The structure of the ruthenium complex dye is as shown in Figure 2.

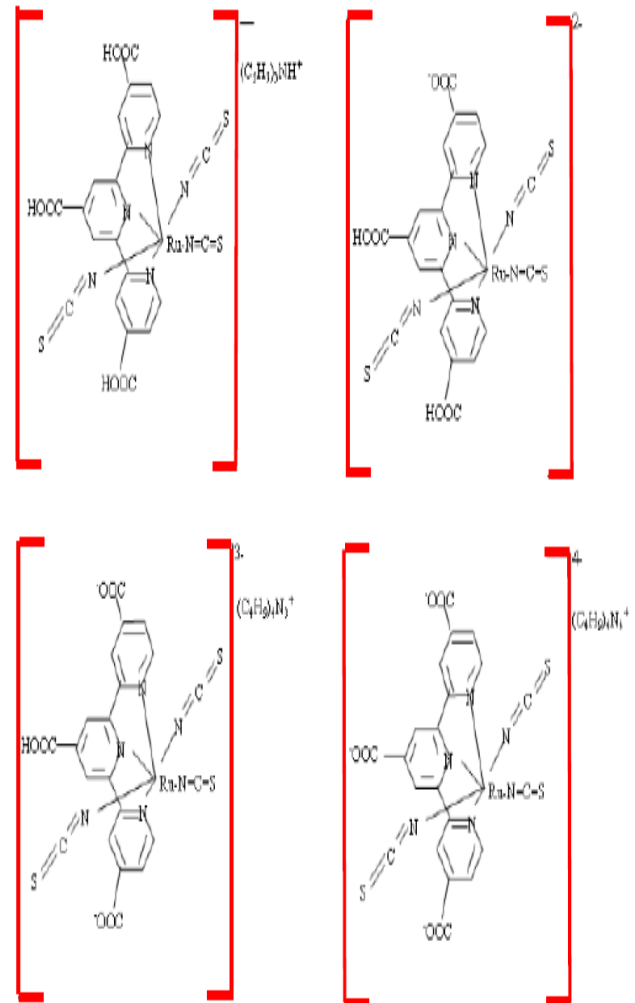


Figure 2. Ruthenium Complex Dye

The combination of the ruthenium dye and the isolated magnetosomes of MTB forms light harvesting trap with the ZnO nanowires. A structure consisting of two-dimensional pattern of a light harvesting system denoted as LH_1 in the

outer shell and LH₂ in the inner shell is developed. These patterns consist of bounded photo-generated excitons transported integrated with magnetite of magnetosomes and driven by the inbuilt magnetic field to the donor acceptor interphase. Here, the LH₁ system and the LH₂ system describes the integral MTB magnetosome proteins with magnetite in which all the generated exciton coupling pigments in the cell are organized regularly following repeated patterns in a circular order. A reaction center with a dense core is surrounded circularly by the light harvesting LH₁ complex. Also the light harvesting LH₂ complexes patterns are arranged orderly around the surface perimeter of LH₁ ring following a 2D repeated structure. The reaction center is located within the center of ring LH₁. In the system there exists over 5000 nanoparticles of magnetite in magnetosomes per enclosed reaction center. Each LH₁ unit is surrounded by over 10 LH₂ discrete units within the complex. Frenkel excitons are generated when light is absorbed following Frenkel's exciton model statistics. Theoretically the photo-generated excitons travel in unique coherent order in the described 2 dimensional light harvesting system to arrive the reaction center under the influence of the magnetic field of the magnetite. In the reaction center, the transition metal ion in the prosthetic group around a protein already is waiting to acquire the photon energy through received excitons to excite and dislocate an electron leading to series of electron transfer complex reaction [22, 23, 24]. The entire photo-generated exciton transport mechanism in the developed silicon solar cell is summarized in Figure 3.

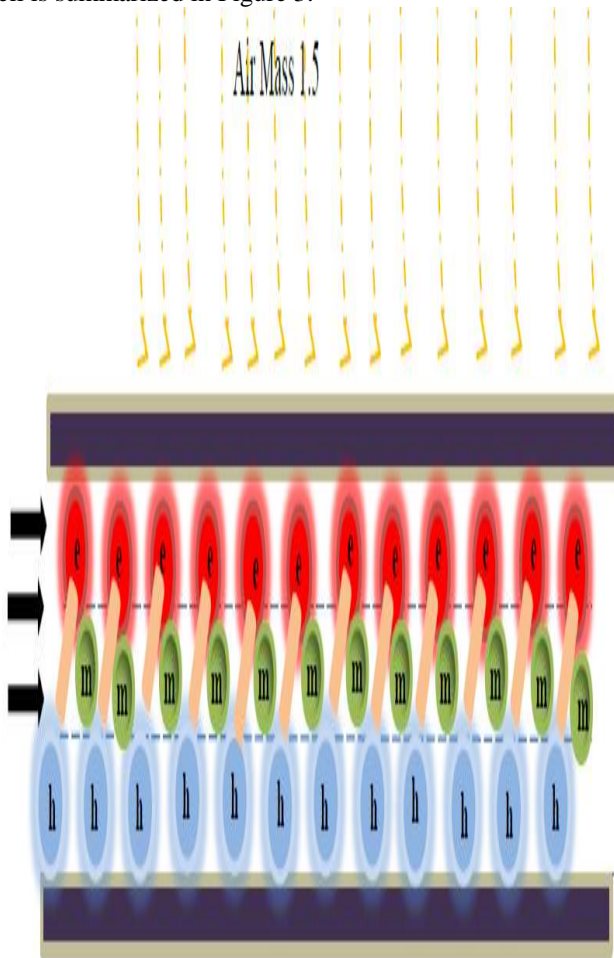


Figure 3. Photo-generated excitons being accelerated under the influence of nanoparticles of magnetite isolated from magnetosomes of Magnetotactic Bacteria.

This novel coherent photo-generated carrier transport mechanism enhanced the solar cell efficiency to a value 13.2%. Also the device achieved temperature stability attributed to the uniformed speedy carrier transport mechanism as shown in Figure 3.

3.0 THEORY / CALCULATION

Solar cells are evaluated by the efficiency in the conversion of incident photons to electrical energy. In order to improve efficiency, emphasis is made on the light absorption of the device, charge transport, charge dissociation, and charge collection within the device minimizing losses in a cost effective manner. Here we consider the following parameters:

$$\eta_{\text{eff}} = \eta_{\text{abs}} \times \eta_{\text{dis}} \times \eta_{\text{trans}} \times \eta_{\text{col}} \quad (1)$$

Where η_{eff} = Total efficiency of Solar Cell

η_{abs} = the light absorption efficiency

η_{dis} = the generated exciton dissociation efficiency

η_{trans} = the charge carrier transport efficiency

η_{col} = the charge collection efficiency

Generally, the key factors of interest in photovoltaic cells performance include the Open Circuit Voltage, Short Circuit Current, Fill Factor, and Maximum Power. The Power Conversion Efficiency (PCE) is defined as the ratio of the Output Power (P_{out}) of the solar cell to its Input Power (P_{in}) given by:

$$\text{Power} = \frac{P_{\text{OUT}}}{P_{\text{IN}}} = \frac{J_{\text{MAX}} V_{\text{MAX}}}{P_{\text{IN}}} = \frac{FF J_{\text{SC}} V_{\text{OC}}}{P_{\text{IN}}} \quad (2)$$

Where J_{MAX} is the Current density at maximum of ($J \times V$)

J_{SC} = the Short circuit current

V_{OC} = the open circuit voltage

FF = the Fill Factor calculated as:

$$FF = \frac{J_m V_m}{J_{\text{SC}} V_{\text{OC}}} \quad (3)$$

The total current voltage response of the solar cell can be approximated as the sum of the generated short circuit photocurrent and the dark current.

The factor termed Incident Photon Conversion Efficiency (ICPE) is defined as the number of photo-generated charge carriers contributing to the photocurrent per incident photon.

4.0 RESULTS AND DISCUSSIONS

The developed Excitonic Photocell was tested with a LabVIEW toolkit at 25°C. The characterization of the solar cell was done at standard conditions (irradiance 1000W/m², Air Mass 1.5). The results are presented in Figure 4 and compared with the result obtained from a Dye Sensitized Solar Cell without MTB under similar conditions in Figure 5. Accordingly, the developed Excitonic Photocell shows a remarkable improvement in the Fill Factor achieving a value 0.81 compared to the Dye Sensitized Solar Cell value of 0.79. Also the device efficiency improved, attaining a value of 13.2% attributed to the enhanced carrier transport.

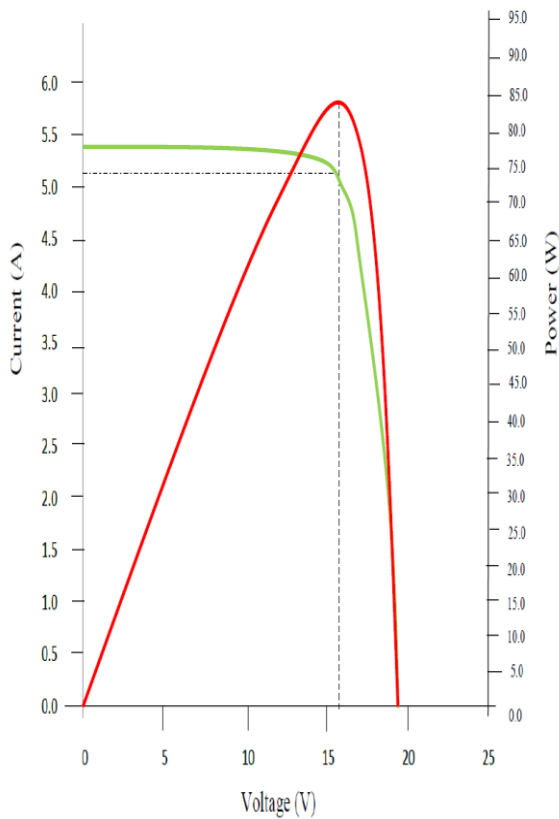


Figure 4. Plot of LabVIEW toolkit VI for characterization of the developed Excitonic Photocell.

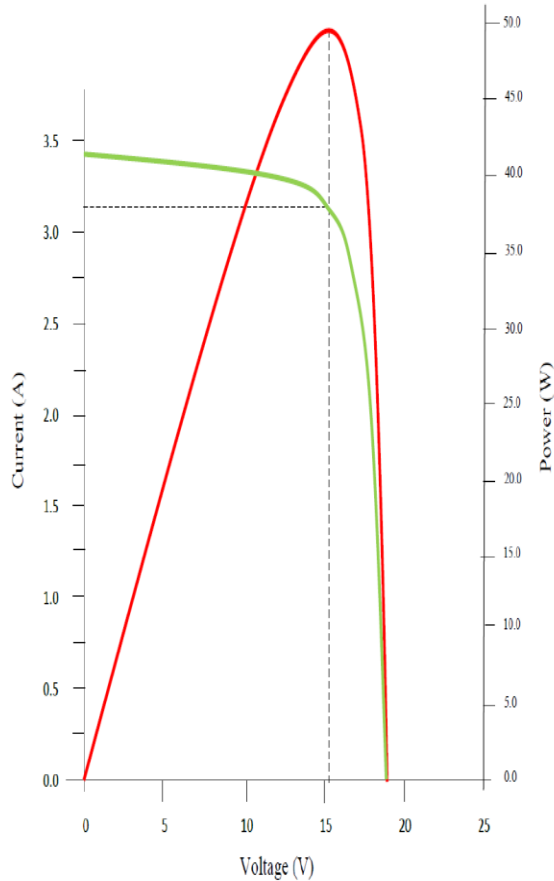


Figure 5. Plot of LabVIEW toolkit VI for characterization photovoltaic solar cell without MTB

The results obtained using the LabVIEW toolkit VI is presented in Table 1 below.

Table 1. LabVIEW toolkit VI results for characterization of the developed Excitonic Photocell compared to dye sensitized solar cell.

Parameter	Developed Excitonic Photocell	Dye sensitized solar cell
Light Intensity (W/m ²)	1000	1000
Photon Absorption Area (m ²)	0.64	0.64
Short circuit current, I _{sc} (Amps)	5.41262	3.35342
Open Circuit Voltage, V _{oc} (Volts)	19.11315	18.17543
Fill Factor, FF	0.816938	0.793154
Maximum Power, P _{max} (watts)	84.51401	48.34263
Maximum Voltage, V _{mp} (Volts)	16.21711	15.3121
Maximum Current, I _{mp} (Amps)	5.21141	3.157152
Efficiency (%)	13.20531	7.55354

The parameters used in the characterization of the device are defined as follows.

Short Circuit Current (I_{sc}): This represents the short circuit condition when the impedance is low and is calculated when the voltage equals zero.

$$I \text{ (at } V = 0) = I_{sc}$$

I_{sc} occurs at the beginning of the forward-bias sweep and is the maximum current value in the power quadrant. In ideal conditions, this maximum current value is the total current (I_t) produced in the device by photon excitation.

$$I_{sc} = I_{MAX} = I_t \text{ for forward bias power quadrant.}$$

Open Circuit Voltage (V_{oc}): This occurs when there is no current passing through the cell.

$$V \text{ (at } I = 0) = V_{oc}$$

V_{oc} is also the maximum voltage difference across the cell for a forward-bias sweep in the power quadrant.

$$V_{oc} = V_{MAX} \text{ for forward-bias power quadrant.}$$

Maximum Power (P_{MAX}), Current at P_{MAX} (I_{MP}) Voltage at P_{MAX} (V_{MP}): The power produced by the device is given by P = VI. At the I_{sc} and V_{oc} points, the power is zero and the maximum value power is between the two points. The voltage and current at this maximum power point are denoted as V_{MP} and I_{MP} respectively.

There are concerns on the effect of temperature on the magnetic properties of magnetite. It is projected that an increase in temperature beyond the termed Curie temperature at (738K), the resultant thermal fluctuations may destroy the normal ferromagnetic alignment feature of magnetic moments in magnetite. This may cause the ferromagnetic strength of the magnetite to diminish. At Curie temperature, the net magnetization of a material drops to zero. But this is unlikely to occur in this case because the temperature of this device can never be elevated to such extreme temperatures during operation. The developed Excitonic Photocell also achieved higher thermostability attributed to the efficient coherent carrier transport mechanism.

5.0 CONCLUSIONS

This research implements a novel technology in the transportation of photo-generated excitons in the solar cell to achieve improved efficiency. The focus of researchers involved in solar cells is gradually shifting away from silicon because of its high fabrication cost and inability of the obtained efficiency to consistently improve with forecast values. Consequently there is need to channel more attention to dye sensitized solar cells and other available technologies. Alternative sources of magnetite like chemical nanoparticles of magnetite have been observed not to have uniformed particle size making them unsuitable for this purpose. There is ongoing research targeted at producing nanoparticles of magnetite with uniformed particle size in a cost effective manner. Furthermore, there are considerations for the application of other dyes besides ruthenium complex like the MK-2 and MK-14 dyes. It is speculated that the efficiency of this device will achieve 50% if combined with other suitable materials.

ACKNOWLEDGMENT

We acknowledge the continued support of the Nanotechnology Laboratory group of Optik Design, Technische Universität Ilmenau, Germany. Our gratitude extends to Prof. Mrs. Ugoji, Microbiology Department, Faculty of Science, University of Lagos, Nigeria for her invaluable contributions throughout the laboratory execution of this project.

References

- [1] Mahmoud A. M., Abu B. M., Norasikin A.L., Amir H.K., and Kamaruzzaman S. "Dye-sensitized solar cells: Development, structure, operation principles, electron kinetics, characterisation, synthesis materials and natural photosensitisers" *Renewable and Sustainable Energy Reviews*. 2016. Vol. 65, pp. 183-213.
- [2] Khan M.Z.H., Al-Mamun M.R., Halder P.K. and Aziz M.A. "Performance improvement of modified dye-sensitized solar cells". *Renewable and Sustainable Energy Reviews*. 2017. Vol. 71, pp. 602-617.
- [3] Peng G., Hoi N., Joel T., and Grätzel. M. "Organic dyes containing fused acenes as building blocks: Optical, electrochemical and photovoltaic properties". *Chinese Chemical Letters*. 2018. Vol. 29, Issue 2, pp. 289-292.
- [4] Change W.C., Chen H.S., Li T.Y. "Highly efficient N-heterocyclic carbene/pyridine-based ruthenium sensitizers: complexes for dye-sensitized solar cells" *Angewandte Chemie*. 2010. Vol. 49, no. 44, pp. 8161-8167.
- [5] Kruger J., Plass R., Gratzel M., Cameron P.J., and Peter L.M. "Charge transport and back reaction in solid-state dye-sensitized solar cells; a study using intensity-modulated photovoltage and photocurrent spectroscopy" *J. Phys. Chem. B*. 2003. Vol. 107. Pp. 7536-7542.
- [6] Naik P., Su R., Elmorsy M.R., El-Shafei A., and Adhikari A.V. "Investigation of new carbazole based metal-free dyes as active photo-sensitizers/co-sensitizers for DSSC's". *Elsevier Dyes and Pigments*. 2018. Vol. 149, pp. 177-187.
- [7] Naik P., Su R., El-Shafei A., and Adhikari A.V. "Improved photovoltaic performances of Ru (II) complex sensitized DSSCs by co-sensitization of carbazole based chromophores" *Elsevier Inorganic Chemistry Communications*. 2017. Vol. 86, pp. 241-245.
- [8] Naik P., Mohamed R.Elmorsy M.R., Su R., Babu D.D., El-Shafei A., and Adhikari A.V., "New carbazole based metal-free organic dyes with D- π -A- π -A architecture for DSSCs: Synthesis, theoretical and cell performance studies". *Elsevier Solar Energy*, 2017. Vol. 153, pp. 600-610.
- [9] Wadman S.H., Kroon J.M., and Bakker K. "Cyclometalated ruthenium complexes for sensitizing nanocrystalline TiO₂ solar cells" *Organic Chemistry & Catalysis*. 2011. Vol. 17. no. 24. Pp. 6781-6790.
- [10] Duerto L., Colom E., Andrés-Castán J.M., Franco S., Garín J., Orduna J. B.Villacampa B., Blesa M.J. "DSSCs based on aniline derivatives functionalized with a *tert*-butyldimethylsilyl group and the effect of the π -spacer". *Elsevier Dyes and Pigments*. 2018. Vol. 148, pp. 61-71.
- [11] Benhattab S., Nakar R., Acosta R.J.W., Berton N., Faure-Vincent J., Bouclé J., Van F.T., and Schmaltz B." Carbazole-based twin molecules as hole-transporting materials in dye-sensitized solar cells". *Elsevier Dyes and Pigments*. 2018. Vol. 151, pp. 238-244.
- [12] Zhu K., Pan H., Li J., Yu-Zhang K., Zhang S, Zhang W., Zhou K., Yue H., Pan Y., Xiao T., and Wu L. "Isolation and characterization of a marine magnetotactic spirillum axenic culture QH-2 from an intertidal zone of the China Sea". *Elsevier Research in Microbiology*. 2010. Vol. 161, no. 4, pp. 276-283.
- [13] Atlas R.M. "Handbook of Microbiological Media. Fourth Edition" 2010. Pp. 994-997.
- [14] Jobin J.J. and Suthindhiran K. "Magnetotactic bacteria and magnetosomes – Scope and challenges". *Elsevier Material Science and Engineering: C*. 2016. Vol. 68, pp. 919-928.
- [15] Oduah U.I. and Yang W. "Advanced Photodetector chip" *IEEE Sensor Journal*. 2016. 10.1109/JSEN.2016.2569821.
- [16] Alkauskas A. and Pasquarello A. "Band-edge problem in the theoretical determination of defect energy levels: the O vacancy in ZnO as a benchmark case" *Physical Review B*. 2011. Vol. 84. Pp. 216-219.
- [17] Ladanov M., Ram M.K., Matthews G., and Kumar A. "Structure and opto-electrochemical properties of ZnO nanowires grown on n-Si substrate" *Langmuir*. 2011, Vol. 27, no. 14. Pp. 9012-9019.
- [18] Chen H.S., Chang W.C., C. and Su C. "Carbene-based ruthenium photosensitizers" *Dalton Transactions*. 2011. Vol. 40. no. 25. Pp. 6765 – 6773.
- [19] Islam A., Singh S.P., Yanagida M., Karim M.R., and Han L. "Amphiphilic ruthenium (II) terpyridine sensitizers with long alkyl chain substituted β -diketonato ligands: an efficient coadsorbent-free dye-sensitized solar cells" *International Journal of Photoenergy*. 2011. Pp.117-119.
- [20] Kisserwan H. and Ghaddar T.H. "Enhancement of photovoltaic performance of a novel dye, "T 18", with ketene thioacetal groups as electron donors for high efficiency dye-sensitized solar cells" *InorganicaChimicaActa*. 2010. Vol. 363, no. 11, pp. 2409-2418.
- [21] Hallett A.J. and Jones J.E. "Purification-free synthesis of a highly efficient ruthenium dye complex for dye-sensitized solar cells (DSSCs)" *Dalton Transactions*. 2011. Vol. 40, no. 15, pp. 3871-3879.
- [22] Fisher, A.C., Peter, L.M., Ponomarev E.A., Walker, A.B. and Wijayantha, K.G.U. "Intensity dependence of the back reaction and transport of electrons in dye-sensitized nanocrystalline TiO₂ solar cells" *Journal Phys. Chem. B*. 2000. Vol. 104, pp. 949-960.
- [23] Wang, P. "A stable quasi-solid-state dye-sensitized solar cell with an amphiphilic ruthenium sensitizer and polymer gel electrolyte". *Nature Mater* 2003. Vol. 2, pp. 402-410.
- [24] Wang P., Wenger B., and Humphry-Baker R. "Charge separation and efficient light energy conversion in sensitized mesoscopic solar cells based on binary ionic liquids" *Journal of the American Chemical Society*. 2005. Vol. 127, no. 18, pp. 6850-6859.